Measurements of Suprathermal Electrons in Hohlraum Plasmas with X-Ray Spectroscopy

S. H. Glenzer,[1] F. B. Rosmej,[2] R. W. Lee,[1] C. A. Back,[1] K. G. Estabrook,[1]
B. J. MacGowan,[1] T. D. Shepard,[1] and R. E. Turner[1]
[1]*L-399, Lawrence Livermore National Laboratory, University of California, P.O. Box 808, Livermore, California 94551*
[2]*Institut für Experimentalphysik V, Ruhr-Universität Bochum, 44780 Bochum, Germany*
(Received 11 August 1997)

Nonthermal excitation of atomic states by suprathermal electrons was observed for the first time within inertial confinement fusion hohlraum plasmas. The nonthermal excitation process results in the simultaneous emission of the Ly-α transition and the K-shell satellite series (lithiumlike through carbonlike) which were observed on temporally resolved x-ray emission spectra. A quantitative analysis with a time-dependent collisional-radiative non-Maxwellian model shows that these spectra can be used to obtain temporally and spatially resolved measurements of the suprathermal electron fraction in indirectly driven inertial confinement fusion targets. [S0031-9007(98)06604-6]

PACS numbers: 52.70.La, 52.25.Nr, 52.25.Vy, 52.58.Ns

Suprathermal electrons can cause degradation in the performance of inertial confinement fusion (ICF) capsules because they preheat the fusion fuel which in turn results in a reduced compressibility of the capsule [1]. For indirect drive experiments, using frequency tripled (3ω) glass lasers to heat a high-Z hohlraum, highly energetic electrons with energies of 20–40 keV are primarily produced by stimulated Raman scattering (SRS) [2–7]. Calculations show that for future ignition experiments, e.g., at the National Ignition Facility, the time-integrated hot electron fraction must be smaller than 15% for 20 keV electrons to avoid a reduction of the capsule gain [1]. Earlier measurements to quantify suprathermal electrons in hohlraums utilized an absolute determination of the Raman scattered light or of the x-ray continuum emission. However, in some cases these techniques can yield ambiguous results as one requires knowledge of the electron velocity distribution [8] and target opacity [9]. Further, these measurements do not give spatially and temporally resolved information, e.g., near the fusion capsule where hot electron measurements are most important. For these reasons it is essential to directly measure hot electrons in fusion plasmas.

In this Letter, we present the first temporally and spatially resolved measurements of the suprathermal electron fraction in ICF hohlraums. These experiments show a clear correlation between the time histories of stimulated Raman scattered light and of the hot electron fraction measured with x-ray spectroscopy [10–13] using titanium tracers mounted at various locations in a gas-filled hohlraum. The presence of highly energetic electrons in these plasmas gives rise to characteristic x-ray emission features showing hydrogenlike resonance emission simultaneously with the emission of Li-, Be-, B-, and C-like satellite lines on temporally resolved spectra. We observe that the intensity of the hydrogenlike resonance transition in Ti ($1s\,^2S$-$2p\,^2P^0$ or Ly-α) is more than 1 order of magnitude larger than calculated for a Maxwellian electron velocity distribution function with a temperature obtained from independent measurements. The analysis of the emission spectra with time-dependent collisional-radiative modeling [14,15] shows that the hot electron fraction peaks about 1 ns after the beginning of the 2.2 ns shaped laser beams. For these experiments, where Nova laser beams without beam smoothing were used, we observe a significant suprathermal electron fraction. The peak fraction is 10% at a distance of about 700 μm from the laser beam spots. The time averaged fraction is 2% which is in agreement with calculations based on measured SRS losses and independent time-integrated filter-fluorescer [9,10] measurements of the suprathermal electron fraction using thin-walled hohlraums [16]. Therefore, these results indicate that the present spectroscopic method is a useful diagnostic for inertial confinement fusion experiments. It is complementary to inner-shell K-α spectroscopy [17] which was applied to measure the (time-integrated) preheat in laser-produced plasmas [18,19]. As pointed out in Refs. [17,19], the possibility of strong self-absorption of the K-α satellites as well as radiation pumping complicates its applicability in high-temperature hohlraum plasmas.

The present experiments were performed at the Nova laser facility [20]. We used cylindrical methane-filled (CH_4) hohlraums that were 2750 μm long with a radius of 800 μm. This is a standard hohlraum that has been used for capsule implosions, drive measurements, and various benchmarking experiments [21–24]. The hohlraums were heated with 2.2 ns long shaped laser beams with a 3:1 contrast and a total energy of up to 27 kJ at 3ω (351 nm) (see below). We applied unsmoothed laser beams resulting in SRS energy losses of about 100 J per beam. The laser beams enter the hohlraum at both ends through laser entrance holes of 600 μm radius covered with 350 nm thick polyimide. They produce a fivefold pattern of elliptical, 700 μm $\times$ 500 μm large laser spots on each side of the hohlraum at a distance of 700 μm from the midplane. The spectroscopic tracer consisting of a mixture of

titanium and chromium 100 μm wide and 200 nm thick was coated on a thin, 300 μm wide CH strip. Two positions of the foil were investigated in detail: a vertical foil crossing the hohlraum axis at a distance of 950 μm from the center so that the foil is not heated by the laser beams [Fig. 1, position (*a*)], but by electron conduction through the CH plasma. The second experiment used vertical foils at the same distance from the center but 400 μm off axis so that the foil is directly heated by two of the laser beams [Fig. 1, position (*b*)].

We observed the titanium x-ray emission of 4.4–5.2 keV (0.28–0.24 nm) spectroscopically with a temporal resolution of 150 ps using a flat crystal spectrometer [25] coupled to a gated microchannel-plate detector using film [26]. Four successive spectra were recorded on a single shot with a time gap of 500 ps between the spectra. In the present study the wavelength resolution is $\Delta\lambda/\lambda \approx 600$.

Figure 2 shows four successive titanium spectra from the foil which is indirectly heated by the gas. In particular we observe at $t = t_0 + 1.1$ ns the hydrogenlike Ly-α transition, the heliumlike resonance line (He-α, i.e., the $1s^2\,{}^1S$-$1s2p\,{}^1P^0$ transition) and intercombination line ($1s^2\,{}^1S$-$1s2p\,{}^3P^0$), the lithiumlike dielectronic satellites ($1s2\ell 2\ell'$-$1s^2 2\ell'$), berylliumlike satellites ($1s2\ell^m 2\ell'^n$-$1s^2 2\ell^m 2\ell'^{n-1}$, $[n + m = 3]$), boronlike satellites ($1s2\ell^m 2\ell'^n$-$1s^2 2\ell^m 2\ell'^{n-1}$, $[n + m = 4]$), and carbonlike satellites ($1s2\ell^m 2\ell'^n$-$1s^2 2\ell^m 2\ell'^{n-1}$, $[n + m = 5]$). As the experimental spectrum is spatially resolved along the height of the foil, we analyze the central, homogeneously emitting part of the foil. All spectra have been corrected for the wavelength-dependent instrument response, filter transmission, and crystal reflectivity.

For a quantitative analysis of the spectra it is necessary to estimate the electron temperature T_e (or 2/3 of the averaged energy) of the thermal electrons. The electron velocity distribution function can be approximated by a cold thermal Maxwellian distribution (T_e) plus a Maxwellian tail of hot electrons ($T_{\rm hot}$) produced by SRS [3]. A standard spectroscopic tool to infer T_e is the line intensity ratio of the He-α intensity to the lithiumlike dielectronic satellites' intensities which are dominated by the *jkl* dielectronic satellites [27]. Extending the analysis of Ref. [28] to the temperature and density regime encountered in this experiment shows that T_e is high enough so that this method is not sensitive to the presence of hot electrons in the plasma. It means that the presence of hot electrons greatly affects the Ly-α emission, but has a negligible effect on the He-α emission. For example, at $t = t_0 + 1.1$ ns this ratio gives $T_e \approx 1$ keV for the titanium-chromium foil plasma. Complete spectra simulations as shown in Fig. 2 and additional measurements of the intensity ratio of the He-β lines from titanium and chromium [29] verify this result. This value is slightly smaller than 1.5 keV of the surrounding CH plasma as measured with Thomson scattering [24], because the heating of the foil lags behind that of the gas.

The comparison of the experimental spectra with collisional-radiative model calculations clearly shows that the experimental spectra are influenced by hot electron excitation. Assuming a single Maxwellian electron velocity distribution with temperatures of 1–1.5 keV results in a calculated relative intensity of the Ly-α transition which is at least 1 order of magnitude smaller than experimentally observed [e.g., the spectrum shown in Fig. 2(b)]. This is demonstrated in Fig. 3 which shows the intensity ratio of the Ly-α lines to the sum of the Be-, B-, and C-like $n = 2$ satellites as a function of the hot electron fraction $f_{\rm hot}^{\ell}$. The calculations are performed for a distribution consisting of two Maxwellians—a thermal Maxwellian of 0.6, 1, or 1.5 keV plus a hot Maxwellian of 19 keV which is consistent with filter-fluorescer [9,10] measurements of

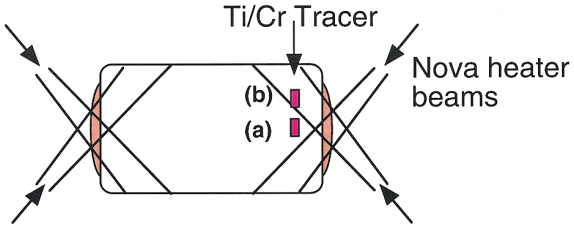

FIG. 1(color). Schematic of a hohlraum target indicating two positions of the spectroscopic tracer. Only spectra from foil position (*a*) were applied to infer the hot electron fraction of the plasma. Spectra from both positions were used to investigate gradients of the electron temperature in the hohlraum.

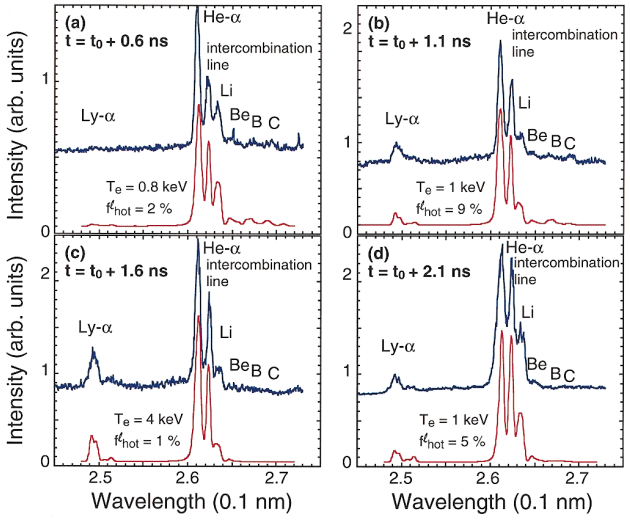

FIG. 2(color). Titanium spectra at $t = t_0 + 0.6$ ns, $t = t_0 + 1.1$ ns, $t = t_0 + 1.6$ ns, and $t = t_0 + 2.1$ ns along with synthetic spectra (lower trace) using time-dependent collisional-radiative modeling [14]. The spectra show the Ly-α spectral lines (0.2491 and 0.2497 nm), the He-α transition (0.261 nm), the intercombination line (0.2623 nm), the lithiumlike satellites (0.264 nm), berylliumlike satellites (0.267 nm), boronlike satellites (0.268 nm), and carbonlike satellites (0.270 nm). The presence of the Ly-α transition at $t = t_0 + 1.1$ ns together with beryllium-, boron-, and carbonlike satellites is due to suprathermal electron excitation.

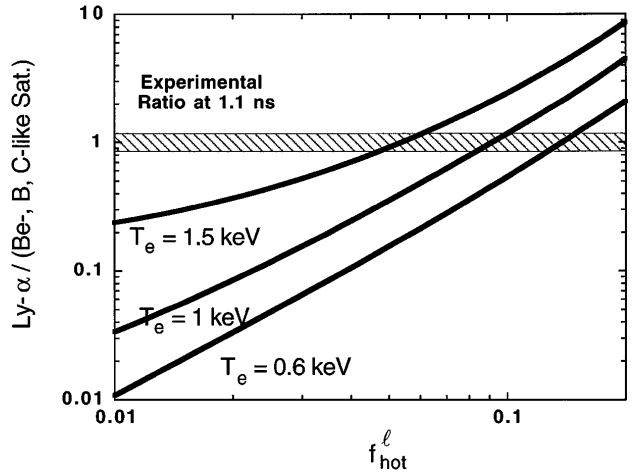

FIG. 3. Intensity ratio of the Ly-α transition to the sum of the Be-, B-, and C-like $n = 2$ K-α satellites as a function of the suprathermal electron fraction. Calculations are shown for an electron velocity distribution function consisting of two Maxwellians with a cold part of 0.6, 1, and 1.5 keV and a hot part with energies of 19 keV. The shaded region indicates the measured ratio at $t = t_0 + 1.1$ ns.

the x-ray bremsstrahlung emission. The electron density is $n_e = 10^{21}$ cm^{-3} and the effective photon path length is $L_{\text{eff}} = 200$ μm. These values are consistent with hydrodynamic simulations of the experiment [30].

The theoretical intensity ratios (Fig. 3) as well as the synthetic spectra (Fig. 2) are calculated with a fully time-dependent collisional-radiative model [14]. It includes optical thickness, (n, L, S, J)-splitting, and highly energetic electrons for the solution of the level populations and subsequent spectral synthesis. Rather than simply causing a shift in the ionization balance, the presence of suprathermal electrons causes a wider distribution of ionization stages at our conditions. For the spectra calculations we define a *local* suprathermal electron fraction

$$f^{\ell}_{\text{hot}} = \frac{n_e(T_{\text{hot}})}{n_e(T_e) + n_e(T_{\text{hot}})}. \quad (1)$$

Here, $n_e(T_e)$ [$n_e(T_{\text{hot}})$] is the number of electrons of the cold (hot) Maxwellian. As the cross sections of the Ti K shell are a weak function of the hot electron energies, the spectrum is sensitive only to the fraction of the hot electrons, not to their energy. We have chosen $T_{\text{hot}} = 19$ keV based on the time-integrated measurements of the bremsstrahlung emission [9,10]. In addition to the spectral lines mentioned earlier the theoretical fits shown in Fig. 1 also include the following unresolved but overlapping transitions: the heliumlike $2\ell 2\ell'$-$1s2\ell'$ and $2\ell 3\ell'$-$1s3\ell'$ transitions, lithiumlike $n = 3$ and $n = 4$ satellites, and nitrogenlike $n = 2$ satellites. Also, the heliumlike $2\ell 2\ell'$-$1s2\ell$ satellites on the red wing of the Ly-α transition are included.

We can justify comparing the emission of the indirectly heated foil [case (*a*) of Fig. 1] with these kinetics calculations because hydrodynamic simulations [30] show that the heating and expansion of the foil is fast enough so that gradients of the foil plasma are not important. That is, for $t = t_0 + 0.3$ ns $< t < t = t_0 + 1.4$ ns, predictions indicate that the foil expands to a diameter of 500 μm with an electron temperature profile which varies by less than 20% over the volume of the foil. However, at $t = t_0 + 1.4$ ns $< t < t = t_0 + 2.2$ ns the foil has expanded significantly reaching colder parts of the hohlraum, then gradients are moderate: the electron temperatures varies by less than 35%. For these later times, uncertainties in the determination of T_e and therefore of the hot electron fraction become larger than for the early time results.

A general good agreement is found between the experimental and synthetic spectra. The comparison (Fig. 2) shows that within the first 0.6 ns of the experiment the foil heats to about 0.8 $\pm$ 0.2 keV. During this initial heating phase the hot electron fraction as inferred from the x-ray spectra is rather small and reaches about (2 $\pm$ 1)%. At $t_0 + 0.6$ ns $< t < t_0 + 1.1$ ns, the SRS power loss measured from a single heater beam increases to 80 GW, and at the same time the hot electron fraction raises to (9 $\pm$ 4)% (Fig. 4) while T_e of the foil plasma is 1 $\pm$ 0.5 keV. For $t > t_0 + 1.1$ ns the power of the heater beams increases significantly, T_e of the foil plasma increases to 4 $\pm$ 1 keV, and the hot electron fraction as well as the SRS losses decrease. Finally, at $t = t_0 + 2.1$ ns the heater beams turn

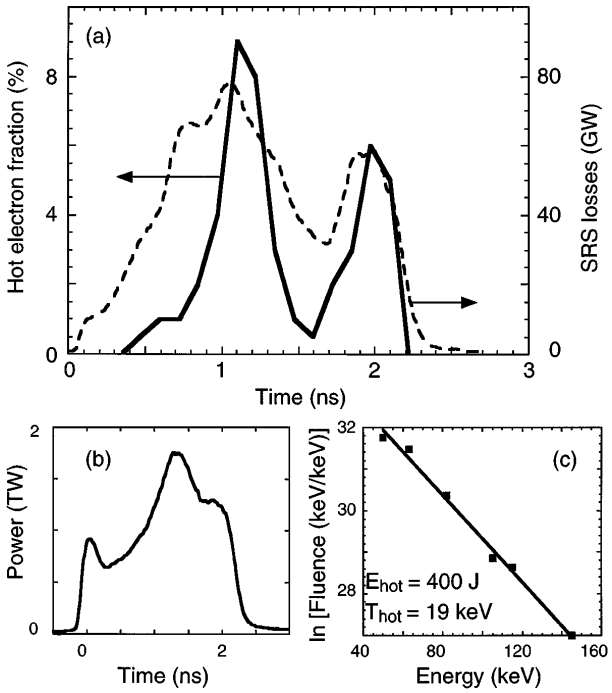

FIG. 4. Suprathermal electron fraction f^{ℓ}_{hot} inferred from the titanium spectra shown in Fig. 2 as a function of time (—). A clear correlation with the SRS losses (- - -) measured from a single heater beam is observed (a). Also shown is the incident laser power from a single heater beam (b) and the time-integrated bremsstrahlung spectrum (c).

off, the temperature further decreases to 1 ± 0.5 keV, and SRS losses and the hot electron fraction diminish. We note that similar data analysis yields 0.5–1 keV higher electron temperatures for the directly heated foil. Thus, the satellite series was not observable and it was not possible to infer the hot electron fraction with reasonable accuracy from these experiments.

Figure 4 shows the temporal evolution of the hot electron fraction inferred from the spectra synthesis. The independently measured SRS losses as well as the incident laser power are shown for comparison. A correlation between the hot electron fraction and the SRS signal is apparent. The error bar for the hot electron fraction is in the range of (25–50)%. Other parameters such as the electron density and opacity are obtained self-consistently from the spectra. They compare well with the results of the hydrodynamic modeling and with calculations based on the initial conditions of the experiments.

A comparison of the temporally integrated hot electron fraction from the spectroscopic measurements shows good agreement with two other methods which were shown to correlate with each other in Ref. [31]. We find from the spectroscopic measurements [Fig. 4(a)]: $1/T \int_0^{2.3\ \mathrm{ns}} f_{\mathrm{hot}}^{\ell}(t)\, dt \cong 0.02$. Assuming that this local value of the hot electron fraction is valid for a large part of the hohlraum plasma and further using an averaged electron density of 10^{21} cm^{-3} from hydrodynamic calculations yields an averaged hot electron energy of 500 J with $f_{\mathrm{hot}} = E_{\mathrm{hot}}/E = 0.019$ from the x-ray spectra ($E =$ 27 kJ the total laser energy delivered to the hohlraum). This value is in close agreement with the temporally and spatially integrating filter fluorescer data shown in Fig. 4(c). They give $E_{\mathrm{hot}} \cong 400J$; $f_{\mathrm{hot}} = 0.015$.

The hot electron fraction and energy can also be estimated from the measurements of the Raman scattered light. From the Manley-Rowe relations we can calculate the energy in suprathermal electrons from SRS [3]. For our conditions we measured a total energy loss into SRS of 1000 J at wavelengths of 460 nm $< \lambda <$ 530 nm. From the hydrodynamic simulations and from the measured SRS spectra we infer that absorption of the Raman scattered light is negligible in these scale-1 hohlraums. Therefore, we can estimate from the measured SRS energy losses a suprathermal electron energy of $E_{\mathrm{hot}} \approx 410$ J which compares well with the above results.

In summary, we have shown that x-ray spectroscopy is a valuable tool to measure the suprathermal electron fraction in fusion plasmas supplementing inner-shell spectroscopy, x-ray continuum measurements, and scattered light measurements. We observe a peak fraction of 10% and a time-integrated fraction of 2% in gas-filled Nova hohlraum plasmas. The time-integrated results agree well with measurements of the x-ray bremsstrahlung emission and with estimates based on measured SRS energy losses. In particular, we observe a clear correlation between the temporally resolved SRS measurements and of the hot electron fraction from x-ray spectroscopy. The present method will be a useful diagnostic for the plasma conditions in future inertial confinement fusion experiments

We thank R. K. Kirkwood for helpful discussions. Partial support was provided by the Deutsche Forschungsgesellschaft under Contract No. Ro 846/6-1. This work was performed under the auspices of the U.S. Department of Energy by the Lawrence Livermore National Laboratory under Contract No. W-7405ENG48.

[1] J. D. Lindl, Phys. Plasmas **2**, 3933 (1995).
[2] J. W. Shaerer *et al.*, Phys. Rev. A **6**, 764 (1972).
[3] K. G. Estabrook *et al.*, Phys. Rev. Lett. **45**, 1399 (1980); K. G. Estabrook and W. L. Kruer, Phys. Fluids **26**, 1892 (1983).
[4] A. A. Offenberger *et al.*, Phys. Rev. Lett. **49**, 371 (1982).
[5] W. L. Kruer, *The Physics of Laser Plasma Interactions* (Addison-Wesley, New York, 1988).
[6] T. P. Hughes, *Plasmas and Laser Light* (John Wiley and Sons, New York, 1975).
[7] B. J. MacGowan *et al.*, Phys. Plasmas **3**, 2029 (1996).
[8] B. B. Afeyan, A. E. Chau, and W. L. Kruer (to be published).
[9] C. L. Wang, Rev. Sci. Instrum. **52**, 1317 (1981); H. N. Kornblum *et al.*, Lawrence Livermore National Laboratory Report No. UCRL-81471, 1978 (unpublished).
[10] R. L. Kauffman, in *Handbook of Plasma Physics*, edited by M. N. Rosenbluth and R. Z. Sagdeev (North-Holland, Amsterdam, 1983); in *Physics of Laser Plasma*, edited by A. Rubenchik and S. Witkowski (North-Holland, Amsterdam, 1991), pp. 111–162.
[11] H. R. Griem, Phys. Fluids B **4**, 2346 (1992).
[12] J. P. Matte *et al.*, Phys. Rev. Lett. **72**, 1208 (1994).
[13] J. Abdallah *et al.*, Phys. Scr. **53**, 705 (1996).
[14] F. B. Rosmej (to be published).
[15] R. W. Lee *et al.*, J. Quant. Spectrosc. Radiat. Transfer **32**, 91 (1984); R. W. Lee (private communication).
[16] N. Delamater *et al.*, Phys. Plasmas **3**, 2202 (1996).
[17] A. Hauer *et al.*, Appl. Opt. **20**, 3477 (1981).
[18] B. Yaakobi *et al.*, Phys. Rev. Lett. **37**, 836 (1976).
[19] J. D. Hares *et al.*, Phys. Rev. Lett. **42**, 1216 (1979).
[20] E. M. Campbell *et al.*, Rev. Sci. Instrum. **57**, 2101 (1986).
[21] B. A. Hammel *et al.*, Phys. Rev. Lett. **70**, 1263 (1993).
[22] R. L. Kauffman *et al.*, Phys. Rev. Lett. **73**, 2320 (1994).
[23] L. J. Suter *et al.*, Phys. Rev. Lett. **73**, 2328 (1994).
[24] S. H. Glenzer *et al.*, Phys. Rev. Lett. **79**, 1277 (1997).
[25] C. A. Back *et al.*, Rev. Sci. Instrum. **66**, 764 (1995).
[26] J. D. Kilkenny, Laser Part. Beams **9**, 49 (1991); F. Ze *et al.*, Rev. Sci. Instrum. **63**, 5124 (1992).
[27] A. H. Gabriel, Mon. Not. R. Astron. Soc. **160**, 99 (1972).
[28] F. B. Rosmej, J. Phys. B **28**, L747 (1995); J. Quant. Spectrosc. Radiat. Transfer **51**, 319 (1994).
[29] C. A. Back *et al.* (to be published).
[30] G. Zimmerman and W. Kruer, Comments Plasma Phys. Controlled Fusion **2**, 85 (1975).
[31] R. P. Drake *et al.*, Phys. Rev. Lett. **53**, 1739 (1984).